

BEM Prediction of Wind Turbine Operation and Performance

Jaya Krishna. M^{*}, Vasishta Bhargava^{**‡}, Dr Jagadeesh Donepudi^{***}

* Department of Mechanical Engineering, GITAM University, Patancheru, Hyderabad

** Department of Mechanical Engineering, Sreyas Institute of Engineering & Technology

***Department of Mechanical Engineering, Narasaraopeta Engineering College, Guntur, A.P

(vasishtab@gmail.com, jayakrishna.m@gitam.in, jagadish.donepudi@gmail.com)

[‡]Corresponding Author; Vasishta Bhargava, Beside Indu Aranya, GSI, Bandlaguda, Nagole, Telangana – 500068

Tel: +91 9502912120, vbhargava@sreyas.ac.in

Received: 1.08.2018, Accepted 05.09.2018

Abstract: For continuous operation and production of energy from wind plants, blades, gearbox, shaft components undergo millions of revolution during the lift time and experience wear and tear due to unsteady aerodynamic forces. During this process the blades need to withstand forces which vary with prevailing wind speed and turbulence at site. In this work boundary element momentum method based numerical computations were performed for horizontal axis 2.1MW pitch controlled, upwind turbine of blade radius 37m. Reduction in blade relative velocity up to 3% is possible at 180^o azimuth position due to the tower effect was observed. A change of less than 1% in blade angle of attack was found for yaw and wind shear effects. The blade angle of attack has been validated using experiment and theoretical results from Gallant, Morote, and Elgamm study. Results showed better agreement near outboard section of blade than inboard region for above rated wind speeds. Data analysis was also conducted for variable speed active pitch regulated 2.1MW wind turbine of rotor diameter 95m and hub height of 80m at a site located in India. The results showed that maximum thrust and power coefficient was found to be 0.951 and 0.447 at wind speeds ~6 m/s and 9 m/s which agreed well with manufacturer's data and computations.

Keywords: Wind turbine, Thrust, BEM, Torque, Power, Wind Speed, Angle of attack

1. Introduction

Wind turbines have been used in past for 1000 years for several purposes such as pumping water, grind grains and produced power by extracting the kinetic energy of wind available in environment [1, 3]. The turbines were smaller in size with rotor diameters less than 10m and operated without any major control mechanisms. Modern large wind turbines however were developed for producing electricity and utilizes advanced technologies to produce dramatically higher energy compared with those existed in ancient or medieval times. Fig.1 shows the various types of wind mills that have been used over the centuries. Modern wind turbines consist of several components and the blades are critical components undergo millions of revolutions in its life time and experience highly unsteady aerodynamic forces during operation that may often lead to

structural component failures of turbine. To monitor the turbine operation and provide preventive steps for failure of components SCADA systems gather data through signals sent by programmable controller placed in a turbine. A power curve is often necessary to track the electric power output or efficiency from a wind turbine in a site as it expresses relationship between the mean wind speed and electric power. The efficiency of such turbine during operation varies with wind speed and turbulence level prevailing at a site and expressed using power and thrust coefficients [1]. In the present work, 2D boundary element momentum method (BEM) is used to determine the aerodynamic forces on the turbine due to its simple approach and low computationally cost. It was first proposed by Glauert in 1926 and based on Rankine-Froude

stream tube model in which fluid is assumed as frictionless incompressible and passes through annular element or disk and represents the rotor [10] Upstream of the rotor disk the stream tube has small cross section than that of downstream. When the air passes through the disk, energy is extracted as a result of change in velocity across the rotor, equal to rate of change of momentum [1, 6] The momentum loss from air stream is converted to aerodynamic torque using finite no of blades which drives the main shaft to produce mechanical torque. BEM is considered most efficient approach in design of blade geometry involving parameters twist, rotor speed, no of blades. The angle of attack seen by blade element provides the necessary lift generated on a blade section. Previous research indicated that sectional rotor efficiency is dependent on optimal angle of attack relative to free stream wind [1, 15] The objective is to present the results from SCADA data analysis for a three bladed active pitch controlled horizontal axis upwind turbine and validate using the manufacturer data for electric power, power (C_p) and thrust (CT) coefficients parameters. The steady BEM computations for angle of attack at different span positions and tip speed ratios has been illustrated and confirmed with the experimental and theoretical values conducted for smaller wind turbines of size $\sim 20kW$. The effect of wind shear and yaw operation on relative velocity of blade and angle of attack is also illustrated for constant wind speed of 8m/s.

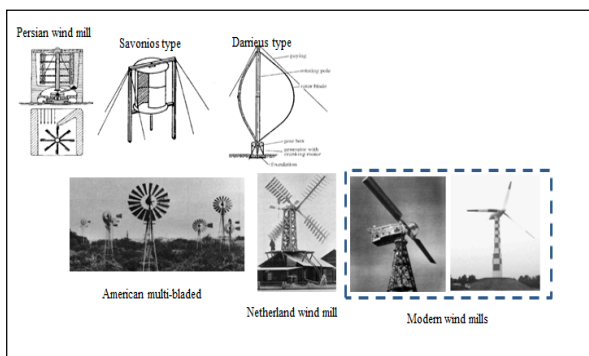


Fig 1 Snapshot of different types of wind mills developed over the ancient, medieval and modern times (source: adapted from [5])

2. Methodology

Albert Betz in his research presented that for frictionless incompressible and non-rotational flows, the theoretical maximum efficiency wind turbines can reach up to 0.593 also known as the Betz limit [1, 3, 5] This limit was derived based on the conservation of mass or continuity equation, momentum and energy principles. The conservation of energy takes account of Bernoulli's

theorem in which the sum of pressure, kinetic and datum heads are kept constant. Since flow was assumed incompressible and arbitrary datum is always constant for wind turbines, both kinetic and pressure heads are utilized in deriving the Betz limit.

2.1 Assumptions of BEM Theory

According to BEM theory flow is assumed steady and each annular element of width dr is independent of other element along blade span. [1, 3, 16] Flow is two dimensional, frictionless and incompressible along the stream tube or rotor disk. Axial induction factor, a , represents the fraction to which air stream slows down in axial direction as it passes through disk. It assumes that there is no wake expansion or rotation of air behind the turbine. During operation, there is no tip losses considered in this model since the rotor is assumed with infinite no of blades [1, 10] However, this assumption is corrected using Prandtl tip factor, F , which assumes rotor as finite no of blades. Further, BEM is designed for axisymmetric flows and the yawing of turbine is not accounted in the analysis of loading on rotor but it can be added into BEM code without significant complexity.

2.2 Turbine aerodynamics

The blade is divided into finite no of discrete annual sections that exchange momentum with air flow and has no radial dependence of flow along the blade length i.e. the relative velocity on one blade section is independent from another. The axial variation in velocity seen by rotor is given by Eq. (1). It represents the change relative to point upstream of rotor. At the rotor disk, it is given by $U_0 (1-a)$ but after passing through the rotor, the velocity reduces further to $U_0 (1-2a)$ using 1D momentum analysis, causing a pressure drop. Figure 2(a) shows the cross section of blade and blade element of width, dr at distance of r from blade root. The pressure drop across the rotor is caused due to difference in free stream velocity upstream and downstream locations of rotor. For simple 1D analysis the induced velocity is considered in only one direction however, for actual operation 2D flow is taken into account including both axial and tangential induction factors. Figure 2(b) illustrates the velocity triangles with direction of resultant aerodynamic force and the blade angle of attack. It is evaluated using the inflow angle seen by blade element and blade twist angle at each section. The resultant velocity, W , seen by blade element is obtained from velocity triangles and given by Eq. (2). The inflow angle is defined as the angle between the apparent velocity at blade element and the angular velocity in rotor plane given by Eq. (3). It varies with local tip speed ratio,

λ_r and induction factors along axial and tangential direction. The lift and drag forces act orthogonal to each other on blade section which is required to produce the necessary torque and thrust during operation and given by Eq.(4) and Eq.(5) where C_L and C_D are the lift and drag coefficients for the blade element or aerofoil profile.

$$a = \frac{U_0 - U_d}{U_0} \quad (1)$$

$$W = U_r = \sqrt{\{(U_0(1-a))\}^2 + \{r\Omega(1+a')\}^2} \quad (2)$$

$$\phi_r = \tan^{-1}\left(\frac{1-a}{(1+a')\lambda_r}\right) \quad (3)$$

$$dF_L = 0.5\rho U_r^2 c_r C_L dr \quad (4)$$

$$dF_D = 0.5\rho U_r^2 c_r C_D dr \quad (5)$$

$$dF_N = dF_L \cos \phi + dF_D \sin \phi \quad (6)$$

$$dF_T = dF_L \sin \phi - dF_D \cos \phi \quad (7)$$

$$dM = dT = [dF_L \sin \phi - dF_D \cos \phi].r \quad (8)$$

$$dA_{Thrust} = 4\pi r a(1-a)U_0^2.r dr \quad (9)$$

$$dA_{Torque} = 4\pi r r \omega a'(1-a)U_0.r^2 dr \quad (10)$$

These aerodynamic forces are then resolved to produce net force in normal and tangential directions of rotor and given by Eq. (6) and Eq. (7). The thrust force acts in direction normal to rotor plane given by Eq. (9) but torque developed is due to tangential force in plane of rotation multiplied by the distance with centre of rotation and given by Eq. (8) and Eq. (10). Further, it can be seen that both thrust and torque for blade element is obtained by resolving aerodynamic forces with respect to inflow angle, ϕ . After obtaining the differential thrust and torque, aerodynamic power of a rotor can be evaluated from the known tip speed ratio, λ . The total aerodynamic power is calculated by integrating the thrust and torque on each blade element along the span. The tip speed ratio of turbine is important operating parameter and a ratio of the blade tip velocity, $R\Omega$, to free stream velocity, U_0 . It must be noted that axial induced velocity acts opposite to free stream velocity on rotor while tangential induced velocity opposite to blade rotation and account for velocity deficit. The induction factors vary along the blade span and at each azimuth position of rotor, decreasing towards the outboard sections. They are obtained after evaluating the normal and tangential force coefficients for each blade section and by rearranging the differential thrust and torque from angular momentum and blade element theory, ignoring higher order or quadratic terms for blade solidity [1, 5]. To account for energy deficit due to wake produced by tip of blade, induction factors are included in BEM implementation using Prandtl tip correction factors [1,3, 5, 6], The modified induction factors serve as the criteria for validity of axial momentum theory which breaks down when axial induction factor, a reaches a value of 0.5 [1, 3, 10]. Further, the efficiency of turbine can be calculated to reach maximum value of 0.593 when a approaches 0.3.

This is also known as Betz limit. The performance of any turbine regardless of size can therefore be summarized using three parameters viz. thrust, torque and power coefficient and given by Eq. (11) – Eq. (13), where B – no of blades, R – blade length. [1, 6, 10]

$$C_T = \frac{F_N}{0.5\rho\pi R^2 U_0^2} \quad (11)$$

$$C_t = \frac{F_T}{0.5\rho\pi R^3 U_0^2} \quad (12)$$

$$C_p = \frac{P}{0.5\rho\pi R^2 U_0^3} = \frac{8}{\lambda^2} \int_0^\lambda a'(1-a)\lambda_r^3 d\lambda_r \quad (13)$$

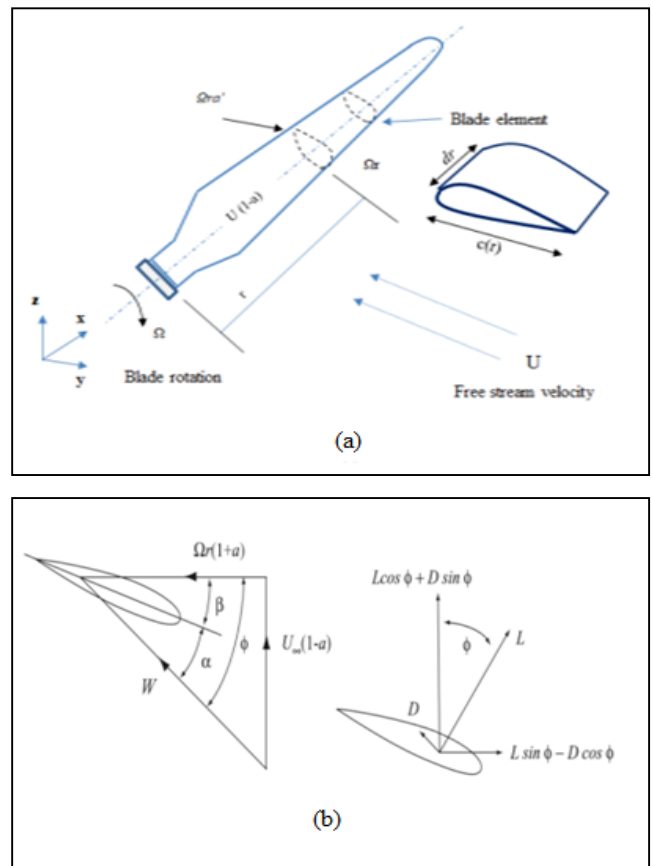


Fig 2 (a) Schematic of wind turbine blade with blade element of width, dr and chord length c , at distance r from root section (adapted from [1]) (b) Velocity triangle representation of aerodynamic forces on blade element [1]

The pitch controlled turbines are operated using programmable controllers which sends the signals to subsystems of turbine involving pitch, yaw actions to track the wind. The rotor speed is measured using a proximity sensor mounted in hub which provides a feedback of rotor revolutions to controller and governs the power output from a turbine. In addition, the controller receives signals from wind speed sensor which is utilized to pitch the

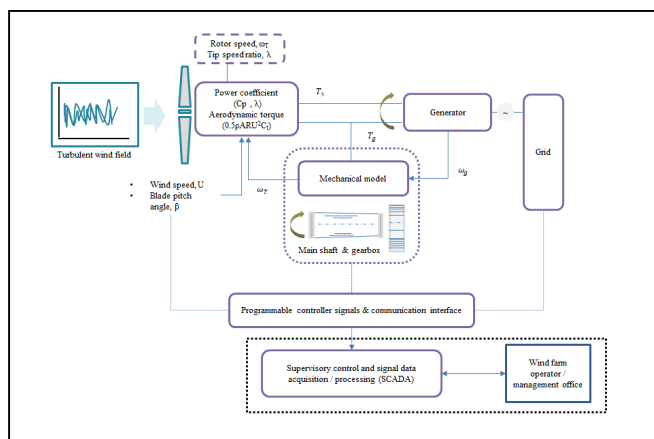


Fig 3 Schematic block diagram of horizontal axis pitch controlled wind turbine model (adapted from [4])

blades in optimal manner. A schematic of turbine integrated with subsystem models along with SCADA interface is shown in Fig 3. Mechanical model uses the main shaft and gearbox, which adapts the rotational speed to account for changing input aerodynamic power for below and above rated wind speeds. The tip speed ratio, λ is continuously varied to keep the optimum output power from turbine. For fixed speed turbines, it occurs at only one wind speed, on the other hand, pitch controlled variable speed turbines track the maximum power output by varying rotational speed constantly for below rated wind speeds and to keep turbine efficiency in optimum manner [1, 20].

3. Results and Discussion

In the present study, the steady BEM computations were done for 2.1MW pitch controlled wind turbine which has following geometry properties as shown in table 1. The flowchart for BEM implementation in MATLAB is illustrated in Fig 4. The solution to BEM based computations depends on cone and tilt angles, as well as geometric properties of blade to determine local angle of attack and resultant velocity. The blades can be pitched into wind which will decrease the angle of attack and reduce the local lift on aerofoil. For pitch controlled turbines, at a given tip speed ratio of rotor, the pitch angle is varied between rated and cut-out wind speeds continuously to keep the output power constant. It can be seen from Fig. 4 that BEM approach uses iterative approach to determine the angle of attack, inflow angle, relative velocity on blade, axial and tangential induction

factors on a given span location of blade. After the induction factors are known, the differential thrust and torque can be calculated using Eq. (9) & Eq. (10). From table 1, the twist and chord properties are higher towards root of the blade than at tip region. For a given rotational speed of turbine, the geometric properties affect the effective angle of attack at blade section, and also the lift force generated. The lift force per unit span for the blade is higher in mid span regions than towards the tip. At the tip of blade the lift coefficient decreases due to formation of vortex caused due to rotation of flow around a closed surface or about a fixed centre. The aerodynamic performance of blade depends on the blade pitching and relative angle of attack, α , which determines the occurrence of stall in inboard sections where the thickness to chord ratios are high. Further, occurrence of boundary layer flow separation on blade caused due to strong adverse pressure gradient is also responsible for reduction in torque and power production [1, 10, 13]. Wind turbine blades are designed in such a way that significant portion of blade undergoes some extent of stall during operation at every wind speed [1, 5, 10].

Table 1. Geometry properties of 37m wind turbine blade

r/R	Chord [m]	Twist [deg]
0.0055	1.93	13
0.1186	3.01	13
0.237	3.22	11
0.3258	2.9	9.5
0.5037	2.15	6.2
0.6814	1.72	3.3
0.7556	1.5	2.3
0.8149	1.4	1.5
0.8742	1.18	0.8
0.9481	0.97	0
0.9868	0.64	2.75
1	0.15	4

The power output from turbine is controlled by dynamic pitching action of blade in stall regulated turbines to prevent generator overloads. The occurrence of dynamic stall for above rated wind speed operation change with rotational effects produced by rotor caused due to boundary layer flow separation. Its effect varies with time dependent interaction of potential and viscous flow over the blade element due to variation in angle of attack. Further, few manufacturers have developed different types of models that include active stall concept by NEG-Micon (now Vestas) and combi stall technology by Siemens. Both concepts use reduced pitch activity and a relatively slow power control compared with active pitch controlled turbines [11].

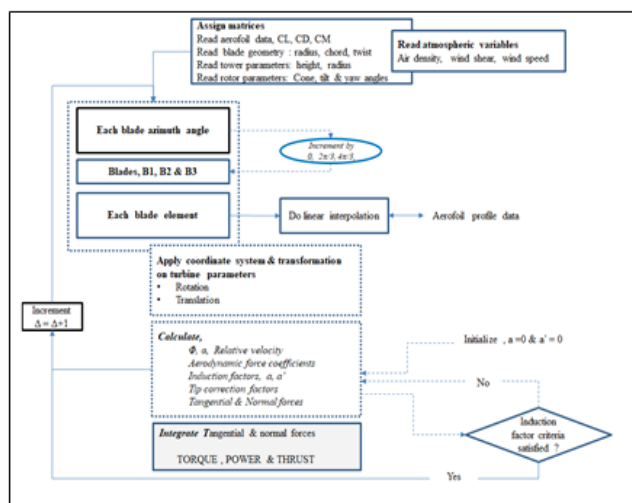


Fig 4 Schematic flow chart of BEM implementation in MATLAB2017b

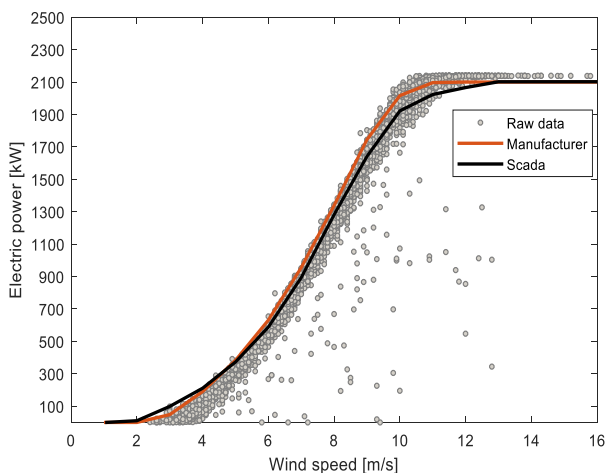
3.1 BEM results

Wind turbines operation at the site depends on prevailing wind field and several studies in the past have shown that wind field is highly turbulent and vary with site factors such as orography [1, 5]. SCADA system ensures that functionality of turbine components are in proper state using time stamped recorded data and by issuing alarm signals. The data is first acquired from site using sensors and processed by software which produces alarm or alert signals to indicate any malfunction situation. Proper sensors functionality is vital for safe operation of wind turbine which enables the wind farm operators to increase the energy production from wind turbines. To achieve this SCADA system continuously processes the information from transducers integrated in a wind turbine controller. Parameters that are essential to turbine operation are wind speed, wind direction, blade pitch angle, yaw angle, rotational speed of rotor and generator, electrical data from generator, temperature and pressure data from hydraulic equipment.

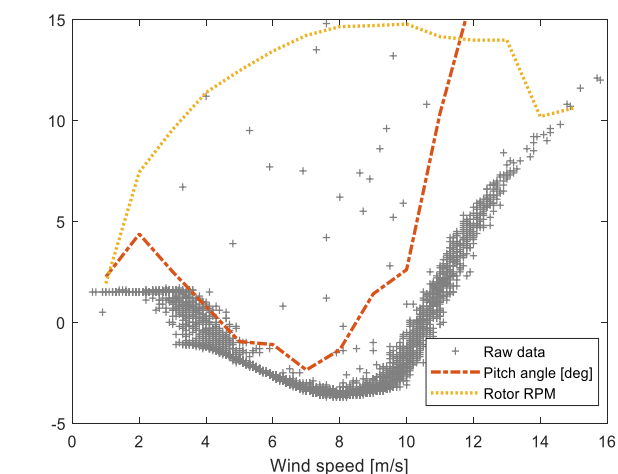
For each parameter, sensor information is sent back and forth between controller and turbine components. Some of them are anemometers for wind speed, wind vane, rotor speed and electric power sensors. During this process SCADA system filters the information in such a way that is suitable for wind farm operators to control the operation of wind turbines in optimal way. In addition, it records the vital information through accelerometers, and position sensors to detect faults and malfunctioning of components which is essential to control O&M costs of turbine. [2, 7, 21] The measured SCADA data contained

4410 data points corresponding to ~735 hours duration. This was reduced for interpreting the results required to be correlated with the manufacturer supplied data. The data reduction was done in two step process. First the data pertaining to each wind speed bin is collated using MS Excel built in logical function to determine the frequency distribution of sampled data points. In the next step, the raw data for electric power, rotor RPM, Ω , blade pitch angle, β and thrust coefficient, CT are filtered using the data validation tool in MS Excel. After performing data binning routine, the final step was to plot the data at each wind speed bin for each of the parameters. It must be noted that SCADA records the data at specific time intervals and averaged typically once in every 10 min duration. The data sampling frequency can be varied using SCADA operator functions however for test certification and accreditation purposes 10 min averaged data is recommended by IEC [1, 7, 11] The data was acquired for site located in geographic coordinates, 27° 8' 0" North, 70° 45' 0" East. Air density corrections were done according to method specified in [1]. In this approach, for variable speed pitch controlled turbines, wind speed and electric power data are corrected based on the rated power of machine. For electric power below 70 % of rated value both air density and electric power corrections are done on data with reference to standard air density. For electric power values higher than 70% rated, only wind speed corrections were done [1]. For both cases it was found to be within ± 1 % of rated values. The power curve obtained from SCADA data has been compared with manufacturer power curve at 1.225 kg/m³. Evidently from Fig. 5(a) the scatter of data between cut-in and rated wind speeds show the power curve from SCADA fits the data points in upper quartile region than the manufacturer power curve. It can be seen that the difference in power produced increased near rated wind speeds however, near cut-tin wind speeds the SCADA power curve is higher compared to standard power curve. The maximum deviation in the linear response region of power curve was found to be ~7.28 % between the SCADA and manufacturer data. The data bins which varied by >10% were considered nonlinear and found at cut-in wind speed bin. Figure 5(b) shows that blade pitch angle for below rated wind speeds is between zero and -5° when the mean rotor speed is rising from 12.1rpm and reach a value of ~15.6 RPM near rated wind speed of 11 m/s. During this regime, the power coefficient, Cp, is kept high by controller and reach value of 0.447 at wind speed of 9m/s. This strategy is common for most pitch controlled turbines in which, controller tries to optimize the Cp value at different tip speed ratios, λ by tracking maximum power until optimal Cp value is obtained. Further from Fig. 5(b) the rotor speed, Ω gains a steady value below rated wind speed and at 10m/s the rotor speed fluctuates due to wind

speed disturbance in site possibly ascertained to change in wind direction. At that point the blade pitch angle is found increasing from 0^0 to $\sim 15^0$ during which power output from turbine is lowered. In the context of pitch controlled turbines, the blade pitch angle is varied constantly to control the rotor speed and not the power output from turbine. [1, 10, 22]



(a)



(b)

Fig 5 (a) Comparison of one month SCADA data for S95-2.1MW with manufacturer power curve and SCADA power curve at 1.115 kg/m^3 (b) Tracking of blade pitch angle, rotor RPM variables using raw SCADA data for S95-2.1MW wind turbine

From Fig 6(a) a comparison of power coefficients for various turbine models was done with increasing rotor diameter. It is clear that turbines with large rotor diameter extract more power at given wind speed. However the power extracted is only advantageous if turbine is equipped with bigger size generator. The rated power is found to reach early compared to turbines with small blade length. In some turbine models there are two generators installed to maximize the conversion efficiency. The

Vestas V-80 2MW and V-82 1.65MW machines have rated wind speeds of 13 m/s and 14 m/s while the S95-2.1MW turbine produced rated power at 11 m/s for type class IEC IIA. [17]. It must be noted that trends for thrust and power coefficients are similar for below rated wind speeds. The maximum value for CT for S95 turbine, from manufacturer data is found to be 0.9568 near the cut-in wind speed of 3.5 m/s while CT from SCADA data analysis was found to be 0.9501 as shown in Fig. 6(b). The CT and Cp values for Vestas V-80, V-82 turbine models reach a value of 0.82, 0.989 and 0.438, 0.4605 respectively while for S95 turbine it was found to be 0.9501 and 0.447. The trends for Cp and CT are validated with those obtained from simulation studies conducted by Fernando & Wu who considered the turbulence effects on wakes from neighbouring wind turbines [9]. The results showed good agreement for above rated wind speeds where turbines operate under high degree of pitching activity limiting the axial thrust force and power outputs from turbine. Since the turbines are pitch controlled the trends were found to be similar irrespective of the size of turbine. Further from Fig 7(a) it can be seen that for S95 model, the average values for CT and torque coefficient (Ct) were in range of 0.338 and 0.0537 and occurred near rated wind speeds. However, the maximum values obtained are ~ 0.9501 and 0.0787 near cut-in wind speeds. The thrust force on rotor was derived using two-step process. First the data binning was performed for electric power, wind speed, and rotational speed variables and in the next step, the torque was obtained using the electric power and rotational speed using the Eq. (11) and applying the bending moment given by Eq. (14).

$$\frac{M}{I} = \frac{\mu}{y} \quad (14)$$

Where I – area moment of inertia of rotor, m^4 , M – Torque developed from rotor, kN-m, μ is the bending stress or the axial aerodynamic thrust force on the blade, y – gravity centre distance along the blade span. Table 2 shows the properties for turbine models used in BEM computation and SCADA analysis. For both models a common hub height assumption and no of blades were chosen. On the other hand, as the hub height is increased, the mean wind speed increases for distances up to 200m from ground. The difference in wind speeds with increase in height causes wind shear. Wind shear in atmospheric boundary layer is measure of velocity gradient and this effect is more dominant for heights above 10m from ground. A representative surface roughness class is often used for wind shear. It is expressed in terms of shear exponent, γ and given by the Eq. (18). In the present study, roughness class 3 and class 5 are used for which wind shear

exponent, $\gamma = 0.1$ and 0.2 . Furthermore, the turbulence intensity in atmosphere affects the measured wind speed and represents overall turbulence [1]. It is function of mean wind speed and expressed ratio of standard deviation of bin averaged wind speed to the free stream velocity given by Eq. (2.6) in ref [1].

Table 2 Main turbine parameters

Turbine parameter	H-2.1MW	S95-2.1MW (SCADA)
Rated output power	2.1MW	2.1MW
Rated wind speed	13m/s	11m/s
Rotor speed	11.7-18.1	12.1-17.6
Rotor diameter	77m	95m
Cone angle	0	2
Tilt angle	4	5
Air density	1.115	1.115
Hub height	80m	80m
# of blades	3	3
Aerofoils	NACA 63-xxx FFA-W3-301, W3-241	Risoe-B

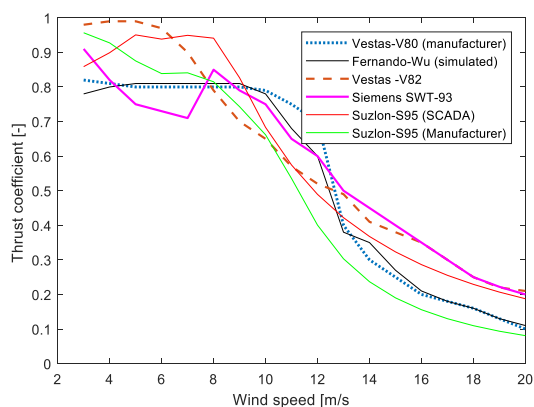
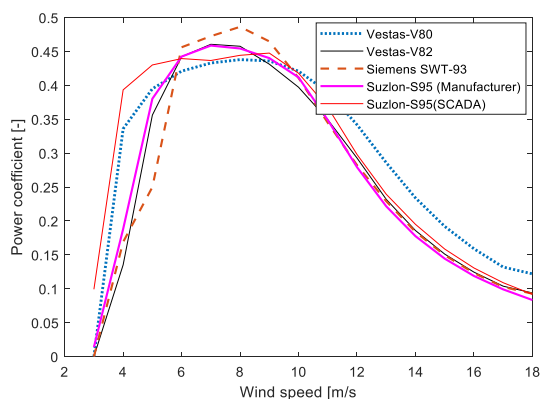
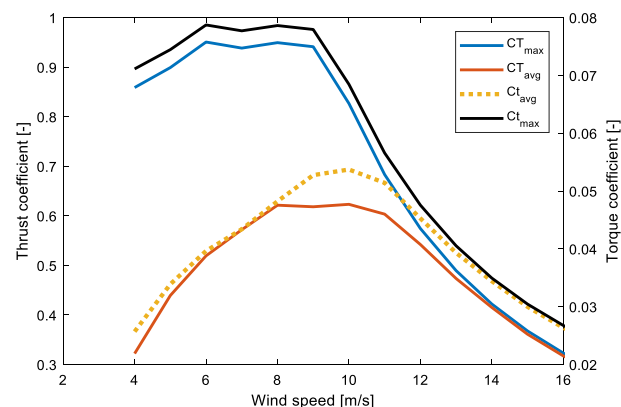


Fig 6 Comparison of (a) power coefficients with SCADA derived data and validated with turbine manufacturers data (b) thrust coefficients derived from SCADA data with various turbine manufacturer data.

It can be seen from Fig 7(b) that turbulence intensity for the site was approximated using the given data period of ~ 1 month and found reducing at higher hub height wind speeds. The standard deviation for each wind speed bin in power curve was found to be ~ 0.25 m/s. At cut-in wind speed, the TI % was found to be 7.5 % which according to IEC and GL turbulence class is considered very low and classified into Class S. The trends agreed with IEC low and high turbulence classes. Also Danish standards specify different turbulence intensity levels with respect to the wind data measured from mast heights between 50m and 120m. Since data analysis was performed with only 1 month data, no conclusion can be made regarding the turbulence type class for this site.

It was noted that at above rated wind speeds the power output from turbine is kept constant using blade pitch angle, β , with leading edge of blade pointing to wind or “pitch to feather” [1, 5, 21, 23] It can be seen from Fig 8(b) that thrust coefficient (CT) computed using steady BEM at wind speed of 8m/s and for blade azimuth positions, $0-240^\circ$ shows that near blade root, the CT values are lower and increase towards outboard elements. The maximum values are found at $0.967r/R$. When the blade reaches 180° position the reduction of CT is found to be $\sim 2\%$ for inboard sections while for outboard sections the reduction in CT was found highest, $\sim 30\%$ with respect to 0° deg. Further, the actual operating conditions of wind turbine in a site also differ significantly from computations due to presence of wakes and surrounding obstacles which affect the overall annual energy production [7]. For large wind turbines, the blade also experiences high Reynolds number of order 1-3 million towards outboard region. The relative velocity on a blade element is high for above rated wind speeds and often result in high unsteady forces due to centrifugal and inertia action of rotor. The pitch controller is highly active for this wind speed regime and torque demand is set to rated value with an aim to lower the high stresses on structural components and improve fatigue life. [1]



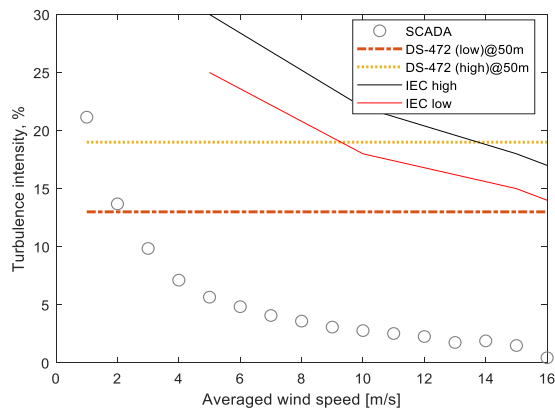
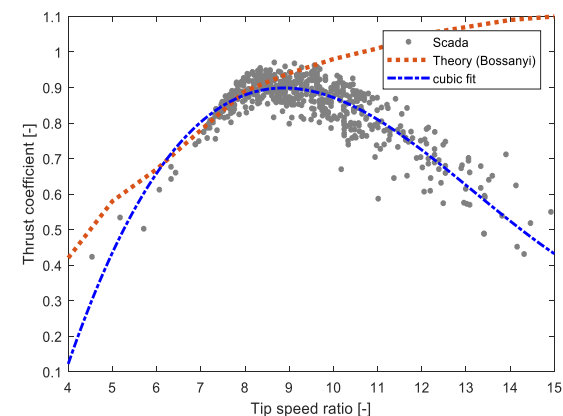
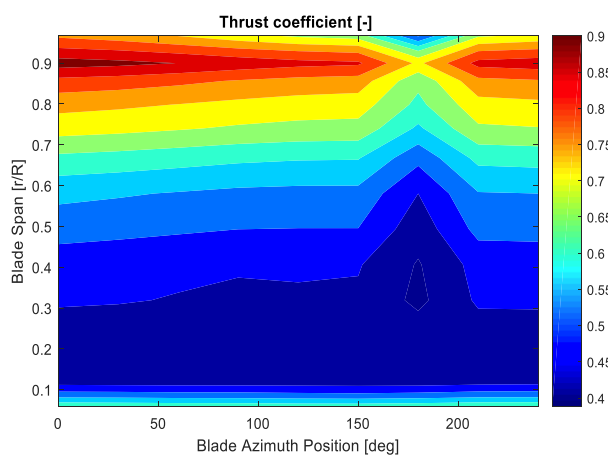


Fig 7 (a) Maximum and average thrust, torque coefficients derived from SCADA data for S95-2.1MW wind turbine (b) Turbulence intensity, % variation with mean wind speeds at a site using SCADA data compared with IEC and Danish standards.



(a)

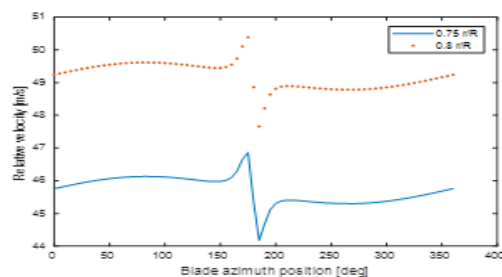


(b)

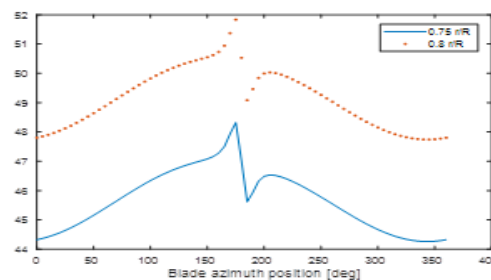
Fig 8 (a) Thrust coefficient [-] for S95-2.1MW turbine from SCADA data with a cubic fit function compared with theoretical prediction [1] (b) BEM computed thrust coefficient for blade azimuth positions between 0 to 240 degrees and at wind speed of 8m/s for $\lambda = 7.6$

3.2 Wind shear & Tower effect

In the section 3.1, it was seen that turbine reached peak thrust coefficient for below rated wind speeds. The thrust force is affected due to relative velocity of blade with respect to free stream velocity. However, it can be noted that the relative velocity is not constant for all blade azimuth positions. For a particular case when the blade position is at 180° fluctuations in velocity are observed as shown in Fig. 9(a). This effect is due to tower which faces the oncoming potential flow and disturbs the relative velocity on blade element. The extent of velocity deficit due to tower is $\sim 3\%$ at $0.75r/R$ and decreases towards outboard elements of blade. This trend is also valid when the turbine is in yaw position as shown in Fig 9(b). The tower effect is modelled using the potential flow seen by cylindrical structure and given by Eq. (15) – Eq. (17) [10]. The radial and tangential velocity components for a point in flow field are obtained by superimposing the streamline function of uniform flow with doublet and vortex strength surrounding the cylinder [18]. For upwind turbines, the rotor is ahead of tower and cause disturbance to the oncoming flow. The rotating blade experiences change in angle of attack at different azimuth positions of rotor. Fig 10 (a) shows the effect of wind shear on blade relative velocity with and without effect of tower with respect to blade azimuth position. In the present study, wind shear exponent of 0.1 and 0.2 representative for extreme and fatigue loads were used to determine the effect of wind shear on blade relative velocity and angle of attack, α .



(a)



(b)

Fig.9 BEM computed blade velocity, m/s at 0.75 r/R, 0.8 r/R, locations for wind speed of 8m/s, when the turbine is in (a) 0° yaw (b) 10° yaw

$$U_r = U_0 \left[1 - \left(\frac{a_t}{x} \right)^2 \right] \cos \theta \quad (15)$$

$$U_\theta = -U_0 \left[1 + \left(\frac{a_t}{x} \right)^2 \right] \sin \theta \quad (16)$$

$$U_y = -U_r \sin \theta - U_\theta \cos \theta \quad (17)$$

$$U_0(x) = U_0(H) \left(\frac{x}{H} \right)^\gamma \quad (18)$$

From Fig. 10(b) the effect of wind shear on angle of attack is shown with and without the effect of tower at TSR of 7.6. For the first case, it is computed using wind shear 0.1 and next with a shear of 0.2. For both cases effect due to wind shear on angle of attack and blade relative velocity were found to vary negligibly.

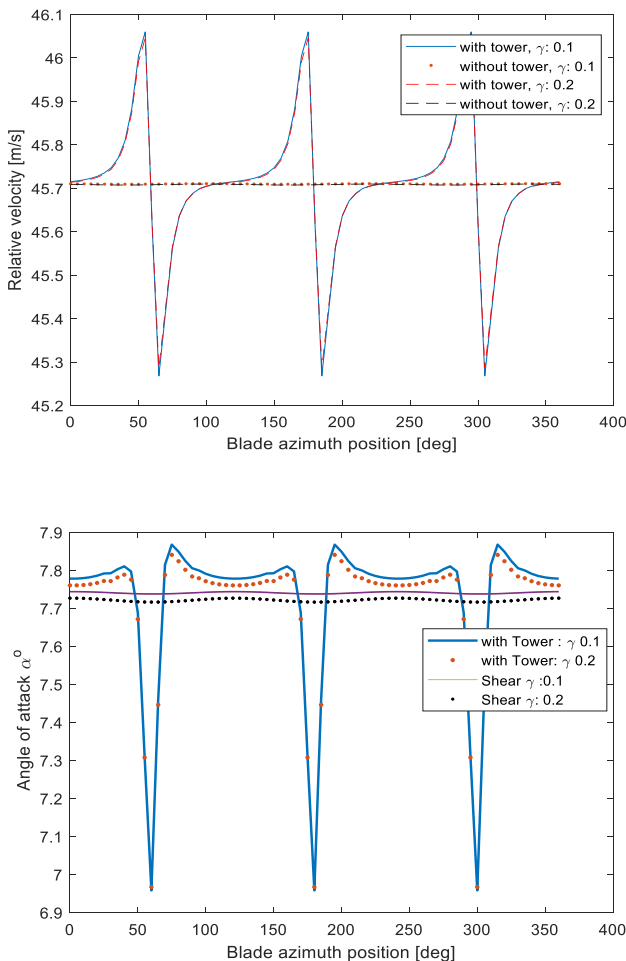


Fig 10 BEM computations for hypothetical 2.1MW turbine at 0° yaw angle, for wind shear of 0.1 and 0.2, at wind speed of 8m/s (a) change in blade relative velocity at 0.75r/R with and without tower effect (b) change in angle of attack at 0.75r/R location with and without tower effect

3.3 Yaw Effect

For pitch or stall controlled turbine, a yaw drive ensures to align the nacelle or rotor blade into direction of wind continuously to extract as much energy as possible to minimize yaw misalignment. During high winds, yaw controller turns the rotor out of wind to limit power extraction. It can be seen that from Fig 11 (a) and 11 (b) the relative velocity and angle of attack has been computed for 0° and 10° yaw positions for turbine including the tower effect. Without considering effect of tower, maximum change in angle of attack and relative velocity can be found when the blade is at 0° azimuth positions and varied by less than 1%. However, if tower effect is included the change is $\sim 2\%$ for both angle of attack, α and blade relative velocity.

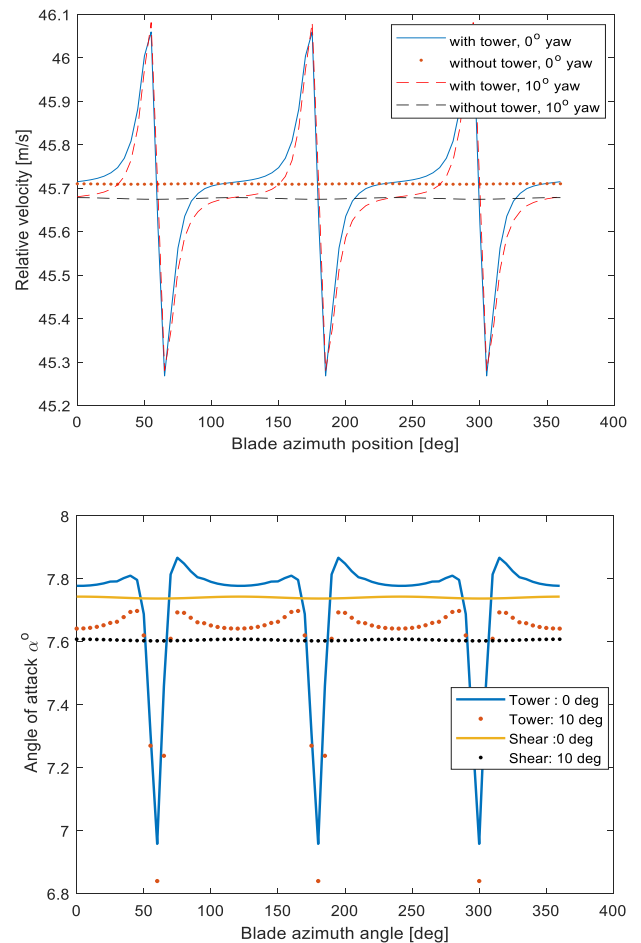


Fig 11 BEM computations for hypothetical 2.1MW turbine at 0° and 10° yaw angle, for $\lambda = 7.6$, constant wind shear of 0.1 and for wind speed of 8m/s (a) change in blade relative velocity at 0.75 r/R with and without tower effect (b) change in angle of attack at 0.75 r/R, with and without tower effect.

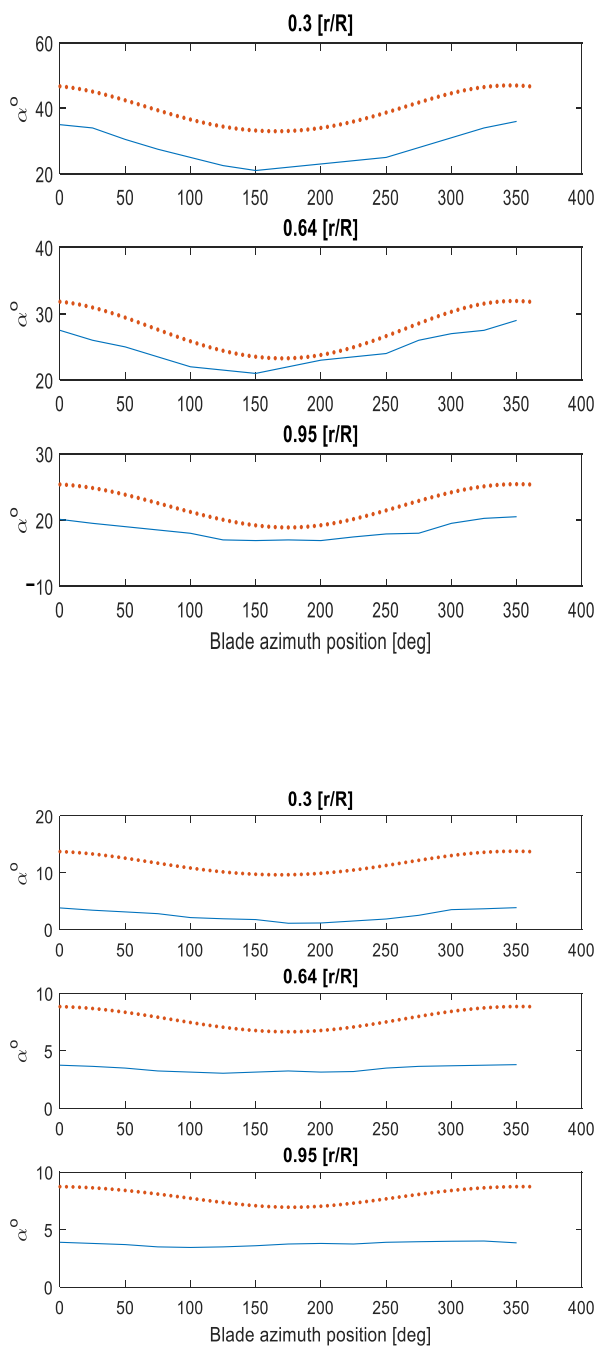


Fig.12 BEM computed blade angle of attack, α^0 , at 0.3 r/R, 0.64 r/R, 0.95r/R locations when the turbine is in 10^0 yaw position (a) at wind speed of 15m/s (TSR-2.6) (b) wind speed of 5 m/s.(TSR -7.6) Red dots indicate the present BEM computations, Blue line show the Elgammi's BEM computation [13].

From Fig. 12(a) the BEM computed angle of attack showed higher deviations, with results from T. Gallant [14] who used three bladed turbine of rotor diameter 1.7m for measuring angle of attack at tip speed ratio of 7.6 or wind speed of 5m/s but agreed well for $\lambda - 2.6$ for above

rated wind speeds. Fig 12 (a) and 12 (b) shows the graph of angle of attack for single blade at 0.3 r/R, 0.65 r/R and 0.95 r/R positions. The physical explanation for the relative velocity perturbation near 180^0 blade azimuth is

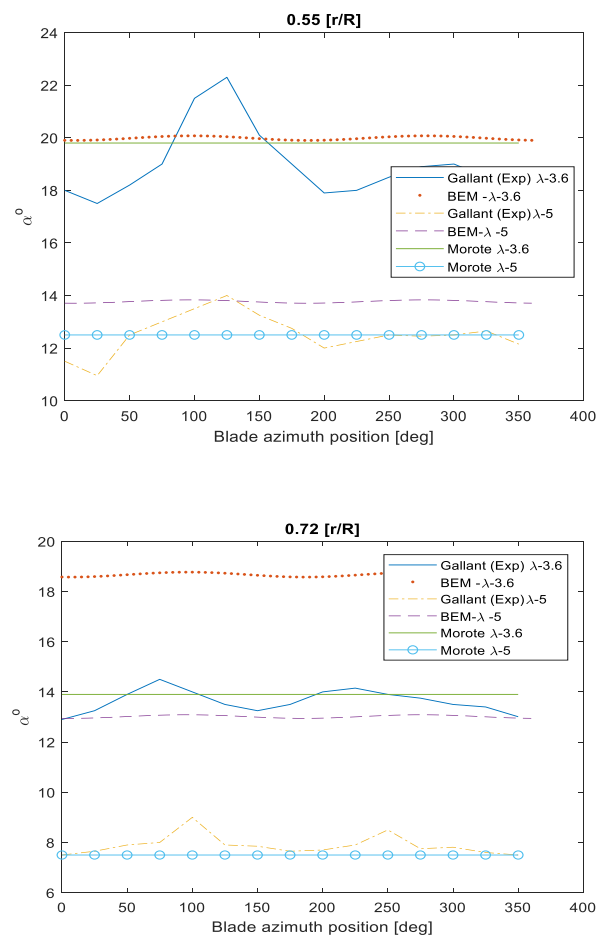


Fig.13 BEM computed blade angle of attack, α^0 , when the turbine is in 0^0 yaw position and wind speed of 10m/s (a) 0.55r/R blade span (b) 0.72r/R blade span

due to turbulent flow separation on blade surface which result in reduced lift and increased torque oscillations [1, 24]. As with the past results conducted by Elgammi and Morote, fairly good correlation exists between the angle of attack and relative velocity on blade element at different span stations [13] In their experimental study, measurements were conducted to analyse the blade angle of attack at two wind speeds, one below the rated, 5m/s and other above rated, 15m/s corresponding to tip speed ratios of 7.6 and 2.6 for a turbine with blade length of ~ 1.7 m. The experiments also included yawing positions at 10^0 , 30^0 and 45^0 . However, for the present BEM computation only 10^0 yaw positions was considered for validation. Figure 13 (a) shows where the angle of attack is computed at different tip speed ratios, $\lambda - 7.6$ and 2.6 for span locations 0.3 r/R, 0.64r/R and 0.95r/R respectively. For micro or small wind turbine blades, the chord and

twist properties are significantly different compared to large blades. Hence deviations for angle of attack, were seen with experiment results from Gallant T and Morote who used two bladed turbine with rotor diameter of 10.1m and 20kW as shown in Fig 13(a) and 13 (b) [14]. Further the deviations were found higher towards the outboard sections for both tip speed ratios than inboard blade element. This shows the trends for angle of attack, and relative velocity using present BEM code agreed well with experiments.

4. Conclusions

The present study investigated aerodynamic performance of pitch controlled horizontal axis wind turbine using SCADA data analysis. The maximum thrust and torque coefficients, CT and Ct, for S95 turbine are found as 0.951 and 0.078 between 6m/s and 8m/s. The power coefficient for S95 model was validated with manufacturer data at 9m/s and showed good agreements. A steady BEM code implementation was performed for hypothetical 2.1MW wind turbine model. The results showed that at higher tip speed ratios, the deviations in angle of attack are higher in outboard regions than inboard sections of blade. BEM computed angle of attack and relative velocity was validated with experiment results of different turbine sizes for all blade azimuth positions and agreed well. The tower and wind shear effect demonstrated that a maximum change in relative velocity was ~3 % at 180° azimuth position and varied by less than 1% for remaining azimuth positions. Effect due to wind shear is negligible on blade relative velocity and angle of attack for all blade azimuth positions.

Nomenclature

Re – Reynolds number
c – Chord length of aerofoil
 U_0 – Free stream velocity
 U_h – Hub height wind speed
 α - Angle of Attack, degrees
L – Span length of aerofoil
 λ - Tip speed ratio, Ω – Rotor speed
R - Blade length
 r – Local blade radius; dr – Local blade width
 ϕ – Inflow angle, β – Blade twist angle
a – Axial induction factor
a' - Tangential induction factor
 μ – Bending stress
B – No of blades
 σ_r – Local blade solidity, σ – Blade solidity factor
F – Prandtl tip loss function
X – Distance of point in wind field to tower centre

U_r – Radial component of free stream velocity
 U_θ – Tangential component of free stream velocity
 a_r – Radius of tower
H – Tower height
x – Distance or height above the ground surface
 γ – Wind shear exponent
BEM – Boundary element momentum
SCADA – Supervisory control and data acquisition
O & M – Operation & Maintenance

References

- [1]. Ervin Bossyanyi. Wind Energy hand book. 1st edition, John Wiley & Sons Ltd (2001)
- [2]. Poul Sorensen et al “Operation and control of large wind turbines and wind farms” DTU orbit. (2005)
- [3]. James Manwell et al. Wind energy explained, Theory, Design and Application, 2nd edition, Wiley eastern publishers. (2010)
- [4]. Ahmed F Zobaa, R.C Bansal. Handbook of renewable Energy technology, World scientific publishing co. ltd. (2011)
- [5]. Gasch. R, Twele. J, Wind power plants, Fundamentals, Design, Construction and Operation, 2nd edition, Springer, (2012)
- [6]. Umesh Chaudhary et al “Modelling and optimal design of small HAWT blades for analysing starting torque behaviour” IEEE publication (2014), doi:// 978-1-4799-5141-3/14/\$31.00,
- [7]. D Astolfi, et al “Wind turbine power curve upgrades” Energies doi: 10.3390/en11051300 (2018)
- [8]. Lei Fu et al “A wind energy generation replication method with wind shear and tower shadow effects” Advances in mechanical engineering, Vol (10) 3 -11. (2018)
- [9]. Yu –Ting Wu, F. Porte Agel “Atmospheric turbulence effects on wind turbine wakes: An LES study”, Energies ISSN1996-1073,5,5340-5362; doi:10.3390/en5125340 (2012)
- [10]. M. Hansen. Aerodynamics of wind turbines, James & James publishers Ltd. (2010)
- [11]. Kenneth et al “Operation and control of large wind turbines and wind farms: Final report”, Risoe national laboratory, Risoe –R – 1532 (EN) (2005)
- [12]. S. Dolan, Peter. W “ Simulation model of wind turbine 3p torque oscillations due to wind shear and tower shadow” IEEE (2006), doi 10.1109/TEC.2006.874211

- [13]. M.Elgammi, Tonio. S “Combining unsteady blade pressure measurements and Free wake vortex model to investigate the cycle to cycle variations in wind turbine aerodynamic blade loads in yaw“
Energies (2016), 9, 460; doi:10.3390/en9060460
- [14]. T. Gallant, D Johnson “ In blade angle of attack measurement and comparison with models”, Journal of physics conference series
(2016). doi:10.1088/1742-6596/753/7/072007
- [15]. F.Hsiao et al “The performance test of three different horizontal axis wind turbine (HAWT) blade shapes using experimental and numerical methods. Energies (2013), 6, 2784-2803; doi:10.3390/en6062784
- [16]. https://en.wikipedia.org/wiki/Blade_element_moment
- [17]. [Environment.govmu.org/English/eia/Documents/Reports/suzlon.../annex8.pdf](http://environment.govmu.org/English/eia/Documents/Reports/suzlon.../annex8.pdf)
- [18]. C.SP Ojha, P.N Chandramouli, R Brendtsson. Fluid mechanics and Machinery, Oxford University Press (2010)
- [19]. <http://gwec.net/publications/global-wind-report-2/gl>
- [20]. Sloomweg , J, E De Vries “Inside wind turbines, fixed vs variable speed”
- [21]. Khalid F Raheem et al. “Wind turbine condition monitoring using Multi sensor data system” International Journal of Renewable Energy Research, Volume 8, Issue 1, March (2018).
- [22]. Astolfo Coronadao et al “Adaptive control of variable speed pitch wind turbines for power regulation” International conference renewable energy research and applications (ICRERA), San Diego, CA, USA (2017)
- [23]. Jae Sung Bae et al “Preliminary study of fabric covered wind turbine blade”. International conference on renewable energy research and applications (ICRERA) Nov (2015) Italy.
- [24]. Abdellah Mohsine et al “Investigation of structural and modal analysis of wind turbine planetary gear using finite element method”, International Journal of Renewable Energy Research, Volume 8, Issue 2, June (2018)